

Superstellar clusters and their impact on their host galaxies.

Guillermo Tenorio-Tagle, Sergiy Silich

*Instituto Nacional de Astrofísica Óptica y Electrónica, AP 51, 72000 Puebla, México;
gtt@inaoep.mx*

Casiana Muñoz-Tuñón

Instituto de Astrofísica de Canarias, E 38200 La Laguna, Tenerife, Spain; cmt@ll.iac.es

ABSTRACT

We review the properties of young superstellar clusters and the impact that their evolution has in their host galaxies. In particular we look at the two different star-forming feedback modes: positive and negative feedback. The development of strong isotropic winds emanating from massive clusters, capable of disrupting the remains of the parental cloud as well as causing the large-scale restructuring of the surrounding ISM, has usually been taken as a negative feedback agent. Here we show the impact that radiative cooling has on the resultant outflows and then, as an extreme example, we infer from the observations of M82 the detailed inner structure of supergalactic winds and define through numerical simulations the ingredients required to match such structures. We also show how when radiative cooling becomes significant within the star cluster volume itself ($\sim 30\%$ of the deposited energy), the force of gravity takes over and drives in situ all the matter deposited by winds and supernovae into several generations of star formation. A situation in which the mass deposition rate \dot{M}_{SC} , instead of causing a wind as in the adiabatic solution, turns into a positive feedback star-forming mode equal to the star formation rate.

1. The properties of superstellar clusters

The discovery by HST of a large population of unusually compact young superstellar clusters (SSCs) within starburst galaxies (see review by Ho 1997; Johnson et al. 2001; Colina et al. 2002; Larsen & Richtler 2000, Kobulnicky & Johnson 1999 and the proceedings edited by Lamers et al. 2004), has led us to infer the unit of massive or violent star formation. SSCs with masses in the range of a few $\times 10^5 M_{\odot}$ to up to $6 \times 10^7 M_{\odot}$ (see Walcher et al. 2004; Pasquali et al. 2004) within a small volume of radius 3 to 10 pc, are indeed some of the

most energetic entities found now in a large variety of galaxies. Note also that collections of them have now been found within a single starburst galaxy, as in M82 and the antennae galaxy (see Melo et al 2005; Whitmore et al. 1999).

The potential impact that these new units of star formation may have on the ISM of their host galaxies has been inferred from cluster synthesis models (see e.g. Cerviño & Mas-Hesse 1994, Leitherer et al 1999). A coeval cluster with $10^6 M_{\odot}$ in stars, an initial mass function (IMF) similar to that proposed by Salpeter and an upper and lower mass range for the coeval event between $100 M_{\odot}$ and $1 M_{\odot}$, leads initially to several tens of thousands of O stars. These however begin to disappear rather quickly (after $t \sim 3$ Myr) as they complete their evolution and explode as supernovae (SNe). The cluster evolution is so rapid that after 10 Myr there are no O stars left within the cluster. All massive stars undergo strong stellar winds and all of them with a mass larger than $8 M_{\odot}$ will end their evolution exploding as supernova. Thus, one is to expect from our hypothetical cluster several tens of thousands of SNe over a time span of some 40 Myr. During the supernova phase a $10^6 M_{\odot}$ stellar cluster will produce an almost constant energy input rate of the order of 10^{40} erg s^{-1} . On the other hand, the ionizing luminosity emanating from the cluster would reach a constant value of 10^{53} photons s^{-1} during the first 3.5 Myr of evolution to then drastically drop (as t^{-5}) as the most massive members of the association explode as supernova. The rapid drop in the ionizing photon flux implies that after 10 Myr of evolution, the *UV* photon output would have fallen by more than two orders of magnitude from its initial value and the HII region that they may have originally produced would have drastically reduced its dimensions. Thus the HII region lifetime is restricted to the first 10 Myr of the evolution and is much shorter than the supernova phase. It is important to realize that only 10% of the stellar mass goes into stars with a mass larger than $10 M_{\odot}$, however, it is this 10% the one that causes all the energetics from the starburst. Being massive, although smaller in number, massive stars also reinsert into the ISM, through their winds and SN explosions, almost 40% of the starburst total original mass. And thus from a starburst with an initial mass of $10^6 M_{\odot}$ one has to expect a total of almost $4 \times 10^5 M_{\odot}$ violently injected back into the ISM, during the 4×10^7 years that the SN phase lasts. From these, almost 40,000 M_{\odot} will be in oxygen ions and less than 1000 M_{\odot} in iron (see Silich et al. 2001).

One of the features of the stellar synthesis models regarding the energetics of coeval star clusters is that they fortunately scale linearly with the mass of the starburst. It is therefore simple to derive the properties of starbursts of different masses, for as long as they present the IMF, metallicity and stars in the same mass range considered by the models.

When dealing with the outflows generated by star clusters, another important intrinsic property is the metallicity of their ejected matter. This is a strongly varying function of time,

bound by the yields from massive stars and their evolution time. Thus, once the cluster IMF and the stellar mass limits are defined, the resultant metallicity of the ejected material is an invariant curve, independent of the cluster mass. Here we consider coeval clusters with a Salpeter IMF, and stars between $100 M_{\odot}$ and $1 M_{\odot}$, as well as the evolutionary tracks with rotation of Maynet & Maeder (2002) and an instantaneous mixing of the recently processed metals with the stellar envelopes of the progenitors (see Silich et al. 2001 and Tenorio-Tagle et al. 2003, for an explicit description of the calculations). This leads to metallicity values (using oxygen as tracer) that rapidly reach $14 Z_{\odot}$ (see Figure 1), and although steadily decaying afterwards, the metallicity remains above solar values for a good deal of the evolution (for more than 20 Myr), to then fall to the original metallicity of the parental cloud, once the oxygen yield has been delivered. One of the main effects of an enhanced metallicity of the ejecta is to boost its radiative cooling and in such a case, massive clusters may inevitably enter into the strong cooling regime, to then find their stationary superwinds totally inhibited (see section 4).

2. Feedback from superstellar clusters

The close spacing between sources within a super-star cluster warrants a very efficient thermalization of all their winds and supernova explosions, leading to the high central overpressure that is to drive both a superbubble and in some cases a supergalactic wind (SGW). The outflow from the star cluster surface is fully defined by three quantities: The mass and mechanical energy deposition rates (hereafter \dot{M}_{SC} and \dot{E}_{SC}) and the radius that encompasses the newly born sources (R_{SC}).

In the adiabatic case, the total mass and energy deposition rates define the temperature and thus the sound speed c_{SC} at the cluster surface.

$$T_{SC} = \frac{0.3\mu}{k} \frac{\dot{E}_{SC}}{\dot{M}_{SC}}, \quad (1)$$

where μ is the mean mass per particle and k the Boltzmann constant. On the other hand, the density of matter streaming out of R_{SC} is:

$$\rho = \frac{\dot{M}_{SC}}{4\pi R_{SC}^2 c_{SC}}, \quad (2)$$

Thus at R_{SC} (see Chevalier & Clegg 1985; hereafter CC85), the ratio of thermal and kinetic energy flux to the total flux is

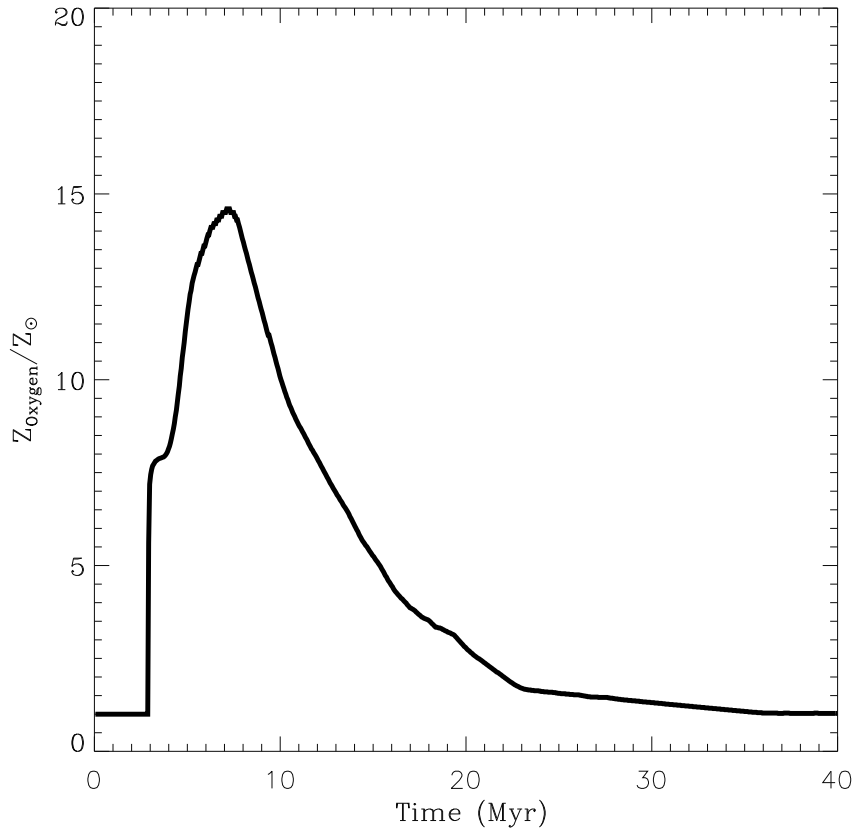


Fig. 1.— The metallicity of the matter ejected by coeval bursts of star formation. The metallicity (in solar units) of the matter reinserted into the ISM by SCs is plotted as a function of the evolution time. The curve is derived from the metal yields of Meynet & Maeder (2002) stellar evolution models with stellar rotation, using oxygen as a tracer. The estimate assumes a Salpeter IMF and $100 M_{\odot}$ and $1 M_{\odot}$ upper and lower mass limits. The model also assumes an instantaneous mixing between the newly processed metals and the envelopes of the progenitors. Note that under these assumptions the curve is independent of the cluster mass.

$$F_{th}/F_{tot} = \frac{\frac{1}{\gamma-1} \frac{P}{\rho}}{\frac{u^2}{2} + \frac{\gamma}{\gamma-1} \frac{P}{\rho}} = \frac{9}{20} \quad (3)$$

$$F_k/F_{tot} = \frac{u^2/2}{\frac{u^2}{2} + \frac{\gamma}{\gamma-1} \frac{P}{\rho}} = \frac{1}{4}. \quad (4)$$

There is however a rapid evolution as matter streams away from the central starburst. After crossing $r = R_{SC}$ the gas is immediately accelerated across the steep pressure gradients and rapidly reaches its terminal velocity ($V_\infty \sim 2c_{SC}$). This is due to a fast conversion of thermal energy, into kinetic energy of the resultant wind.

In a recent communication (Silich et al. 2003, 2004), we have revised the properties of SSCs by solving the flow equations without the assumption of an adiabatic flow made by Chevalier & Clegg (1985). In this case, the steady-state solution results from solving

$$\frac{1}{r^2} \frac{d}{dr} (\rho u r^2) = q_m, \quad (5)$$

$$\rho u \frac{du}{dr} = -\frac{dP}{dr} - q_m u \quad (6)$$

$$\frac{1}{r^2} \frac{d}{dr} \left[\rho u r^2 \left(\frac{u^2}{2} + \frac{\gamma}{\gamma-1} \frac{P}{\rho} \right) \right] = q_e - Q, \quad (7)$$

where q_e and q_m are the energy and mass deposition rates per unit volume ($q_e = q_m = 0$ if r exceeds R_{SC}), Q is the cooling rate ($Q = n^2 \Lambda$) where n is the wind number density and Λ is the cooling function (a function of T and metallicity). Central values of density and temperature are found by iteration, with the restriction that the flow velocity ought to increase from 0 km s⁻¹ at the cluster center to the sound speed when it reaches the cluster surface. If this happens then the stationary solution is fully warranted. A solution in which what is put in (\dot{M}_{SC}) is at all times equal to the outflow from the star cluster surface ($4 \pi R_{SC}^2 \rho_{SC} c_{SC}$). Radiative cooling leaves almost unaffected the wind density and velocity distributions but its temperature may for energetic clusters fall rapidly to $T \sim 10^4$ K, close to the SSC surface. Figure 2 compares the adiabatic (dotted lines) with the radiative solution (solid lines) for a cluster with a $\dot{E}_{SC} = 3 \times 10^{41}$ erg s⁻¹, in which the wind temperature instead of steadily falling as $r^{-4/3}$, it rapidly falls to $T \sim 10^4$ K, reducing drastically the size of the resultant X-ray emitting volume. The energetic winds lead to a total restructuring of the surrounding ISM, and in some extreme cases their energetics may even reach the outskirts of a galaxy causing a galactic wind.

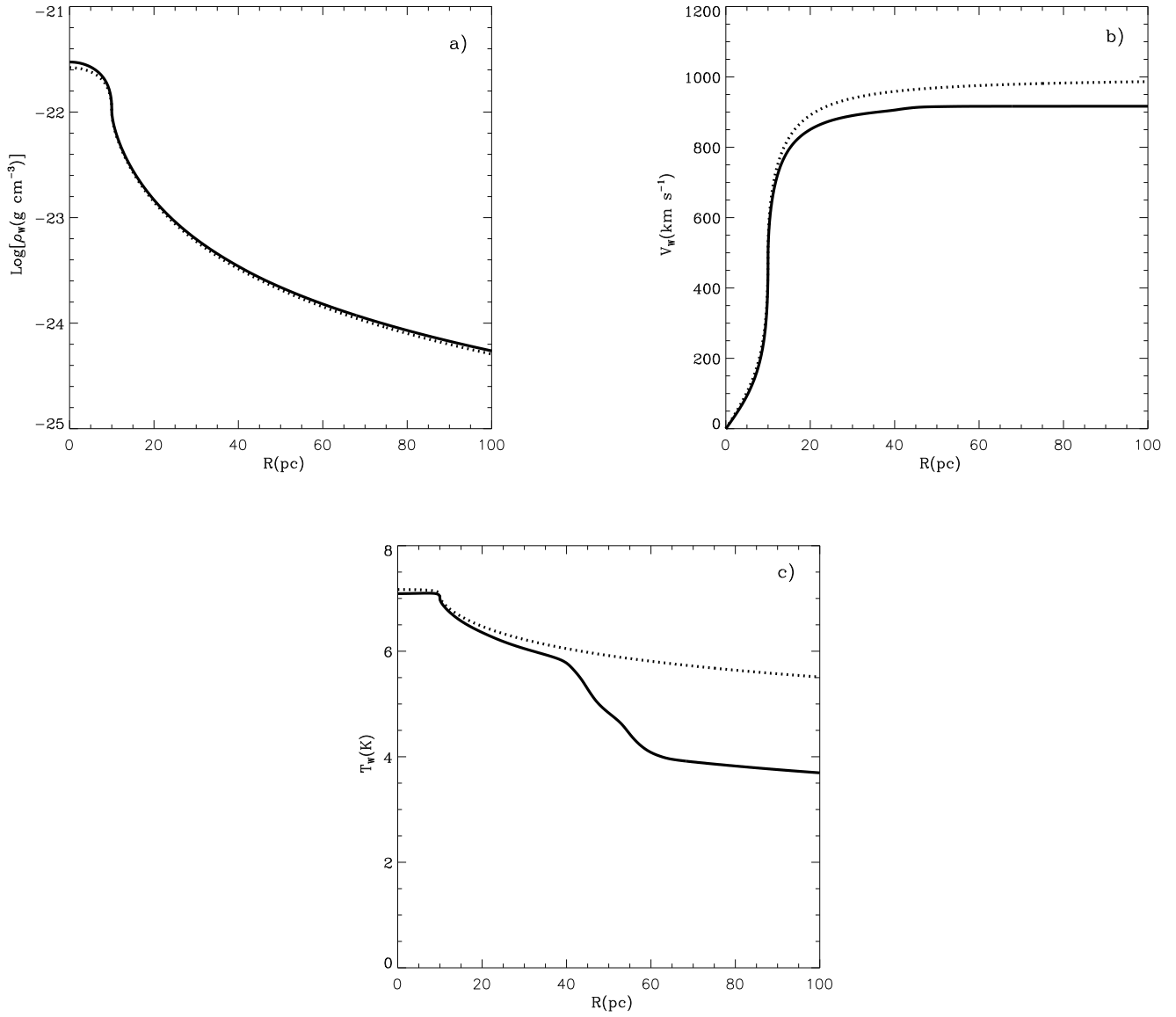


Fig. 2.— Adiabatic vs radiative superwinds. Density, velocity and temperature distributions of the wind produced by a 10 pc radius SSC that deposits $3 \times 10^{41} \text{ erg s}^{-1}$ under the adiabatic (dotted lines) and radiative (solid lines) assumptions.

We have also shown (see below section 4) that in the \dot{E}_{SC} vs star cluster radius diagram, there is a threshold limit that massive and energetic compact clusters may cross to find out that radiative cooling inhibits their stationary outflow condition (Silich et al., 2004) and then the matter ejected by the stellar sources, unable to escape, is to accumulate within the star cluster volume (see section 4).

3. Negative feedback and the physics of supergalactic winds

In all cases below the threshold line, which may be considered quasi-adiabatic or strongly radiative, the energy dumped by the central starburst, is to cause a major impact on the surrounding gas. The supersonic stream leads immediately to a leading shock able to heat, accelerate and sweep all the overtaken material into a fast expanding shell. In this way, as the whole structure grows, the density, temperature and thermal pressure of the wind drops as r^{-2} , $r^{-4/3}$ and $r^{-10/3}$, respectively (CC85).

Note however that such a flow is exposed to the appearance of reverse shocks whenever it meets an obstacle cloud or when its thermal pressure becomes lower than that of the surrounding gas, as it is the case in strongly radiative winds and within superbubbles. There, the high pressure acquired by the swept up ISM becomes larger than that of the freely expanding ejecta (the free wind region; FWR), where ρ , T and P are rapidly falling. The situation leads to the development of a reverse shock and with it to the thermalization of the wind kinetic energy, reducing the size of the free-wind region. Thus for the FWR to extend up to large distances away from the host galaxy, the shocks would have had to evolve and displace all the ISM, leading to a free path into the intergalactic medium through which the free wind may flow as a supergalactic wind. The energy required to achieve such a task, depends strongly on the ISM density distribution. As shown by Silich & Tenorio-Tagle (2001) the energy required to burst into the inter-galactic medium out of a fast rotating flattened galaxy is orders of magnitude smaller than that required to exceed the dimensions of a slow rotating and more spherical density distribution (see Figure 3).

Given their large UV photon output and mechanical energy input rate, SSCs are now believed to be the most powerful negative feedback agents in starburst galaxies, leading not only to a large-scale structuring of the ISM and to limit star formation, but also to be the agents capable of establishing as in M82 a supergalactic wind, thereby removing processed material from galaxies and causing the contamination of the IGM (Tenorio-Tagle et al. 2003).

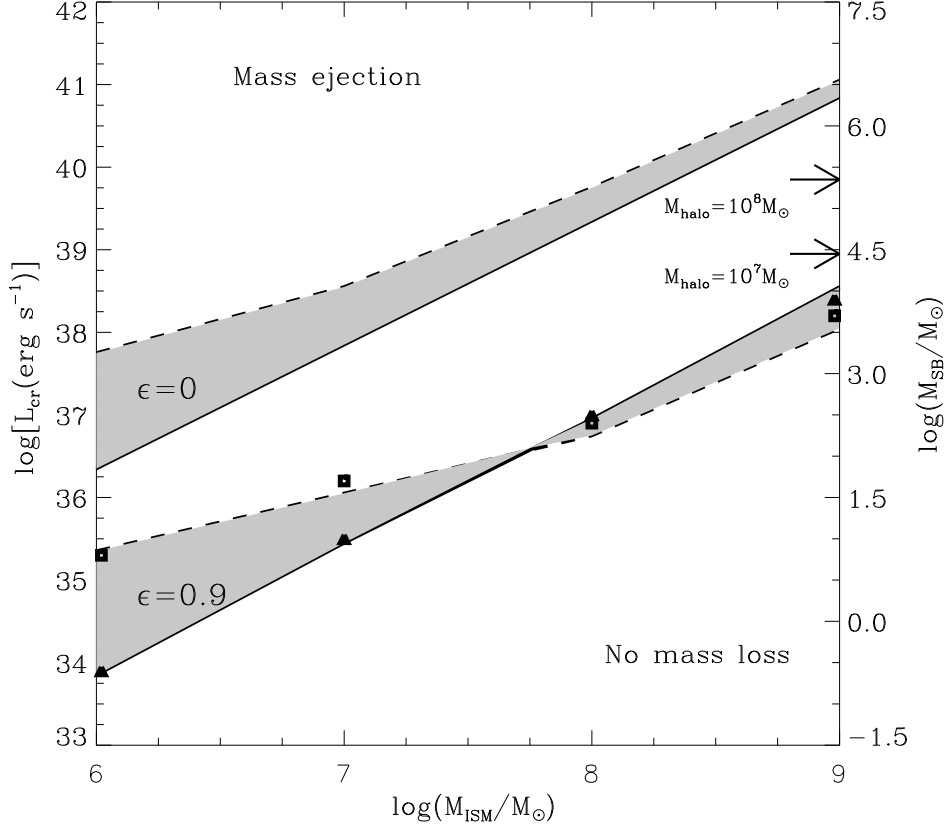


Fig. 3.— Energy estimates. The log of the critical mechanical luminosity, and of the starburst mass (right-hand axis), required to eject matter from galaxies with a M_{ISM} in the range $10^6 - 10^9 M_{\odot}$. The lower limit estimates are shown for galaxies with extreme values of rotation (typical of spirals) and for two values of the intergalactic pressure $P_{\text{IGM}}/k = 1 \text{ cm}^{-3} \text{ K}$ (solid lines) and $P_{\text{IGM}}/k = 100 \text{ cm}^{-3} \text{ K}$ (dashed lines). The upper limit estimates are for galaxies without rotation and thus presenting an almost spherical mass distribution. The resolution of our numerical search is $\Delta \log L_{\text{cr}} = 0.1$. Each line should be considered separately as they divide the parameter space into two distinct regions: a region of no mass loss (below the line) and a region in which blowout and mass ejection occurs (above the line). Also indicated on the right-hand axis are the energy input rates required for a remnant to reach the outer boundary of a halo with mass $10^8 M_{\odot}$ and one with mass $10^7 M_{\odot}$, for the case of a gravitational potential provided by $M_{\text{DM}} = 9.1 \times 10^9 M_{\odot}$ that can hold an $M_{\text{ISM}} = 10^9 M_{\odot}$. The filled squares and triangles represent analytical energy input rate estimates.

3.1. The inner structure of M82

The biconical outflow of M82, the nearest example of a supergalactic wind (SGW), displays a collection of kpc long optical filaments embedded into an even more extended pool of soft X-ray emission. The outflow is known to extend even further, reaching the “H α cap” at 11 kpc from the nucleus of M82 (see Devine & Bally 1999). Both features have been partly explained either with the results of Chevalier & Clegg (1985) model of an adiabatic, freely expanding, stationary wind and/or by the remnant of a large-scale superbubble evolving into the ISM and the halo of the galaxy (see for example Suchkov et al. 1994). Both explanations, based on the energetics of a single stellar cluster, fail to explain the detailed inner structure of the outflow. The elongated filaments for example, are now known to emanate from the central starburst and are not the result of a limb brightened superbubble outer structure (Ohyama et al 2002). Note also that the filaments cannot be reconcile with instabilities in the large-scale supershell, driven by matter entrainment, which in the models occurs at large distances, kpc from the energy source. Furthermore, the stationary superwind solution of Chevalier & Clegg leads to a laminar flow and not to gas condensation or to a filamentary structure at all. Also, as shown by Strickland & Stevens (2000) it has failed to matched the X-ray luminosity of the M82 superwind. Note also that the adiabatic assumption, central in the model of Chevalier & Clegg, has recently been shown to be inapplicable in the case of massive and concentrated starbursts (Silich et al. 2003, 2004). Another important issue not accounted by most of the numerical simulations is the size of the waist of the biconical structure (150 pc radius in the case of M82), which in all calculated cases under the assumption of a single source of energy, (perhaps with the only exception of Tenorio-Tagle & Muñoz-Tuñón 1997, 1998, which account for the infall of matter into the central starburst), also end up with a remnant that presents a wide open waist along the galaxy plane (see figures in Tomisaka & Ikeuchi, 1988; Suchkov et al., 1994). Further arguments regarding the disagreement between theory and observations are given in Strickland & Stevens 2000, Strickland, Ponman & Stevens 1997, and in Tenorio-Tagle et al. 2003.

3.2. The physics of supergalactic winds

So far, all calculations in the literature have assumed that the energy deposition arises from a single central cluster that spans several tens of pc, the typical size of a starburst. Following however, the indisputable observational findings with HST, we have recently made the first attempt to calculate the hydrodynamics that result from the interaction of the winds from neighboring young compact clusters present in a galaxy nucleus (see Tenorio-Tagle et

al 2003). Several aspects were considered in our two dimensional approach to the problem. Among these, the metallicity of the superwind matter was shown to have a profound impact on the inner structure of supergalactic winds. Full three dimensional calculations of the interaction of multiple SSC winds are now underway.

Several two dimensional calculations using as initial condition CC85 adiabatic flows have been performed with the explicit Eulerian finite difference code described by Tenorio-Tagle & Muñoz-Tuñón (1997, 1998). This has been adapted to allow for the continuous injection of multiple winds (see below).

We have considered the winds from several identical SSCs, each with a mechanical energy deposition rate equal to 10^{40} erg s^{-1} . The energy is dumped at every time step within the central 5 pc of each of the sources following the adiabatic solution of Chevalier & Clegg (1985). The time dependent calculations do not consider thermal conductivity but do account for radiative cooling, with a cooling law (Raymond et al. 1976) scaled to the metallicity assumed for every case.

Figure 4 presents the results for which the assumed metallicity of the winds was set equal to $10Z_{\odot}$, justified by the high metallicity outflows expected from massive bursts of star formation (see Figure 1). The winds from the SSCs are exposed to suffer multiple interactions with neighboring winds and are also exposed to radiative cooling. For the former, the issue is the separation between neighboring sources and for the latter the local values of density, temperature and metallicity. Radiative cooling would preferably impact the more powerful and more compact sources, leading to cold ($T \sim 10^4$ K) highly supersonic streams.

Figure 4 shows three equally powerful ($L_{SC} = 10^{40}$ erg s^{-1}) superstellar clusters sitting at 0, 60 and 90 pc from the symmetry axis. All of them with an $R_{SC} = 5$ pc, produce almost immediately a stream with a terminal velocity equal to 1000 km s^{-1} . At $t = 0$ yr the three clusters are embedded in a uniform low density ($\rho = 10^{-26}$ g cm^{-3}) medium. Thus our calculations do not address the development of a superbubble, nor the phenomenon of breakout from a galaxy disk or the halo, into the IGM. The initial condition assumes that prior events have evacuated the region surrounding the superstellar clusters, and we have centered our attention on the interaction of the supersonic outflows.

Figure 4 shows the development of a SGW until it reaches dimensions of one kpc, together with the final temperature structure splitted into the four temperature regimes: The regime of H recombination 10^4 K - 10^5 K, followed by two regimes of soft X-ray emission 10^5 K - 10^6 K, and 10^6 K - 10^7 K and the hard X-ray emitting gas with temperatures between 10^7 K - 10^8 K.

The crowding of the isocontours in the figures indicates steep gradient both in density

Fig. 4.— Two dimensional superwinds. The first four panels represent cross-sectional cuts along the computational grid showing: isodensity contours with a separation $\Delta \log \rho = 0.1$ and the velocity field for which the longest arrow represents 10^3 km s^{-1} . The following four panels display isotherm contours, within the range $10^4 \text{ K} - 10^5 \text{ K}$, $10^5 \text{ K} - 10^6 \text{ K}$, $10^6 \text{ K} - 10^7 \text{ K}$ and $10^7 \text{ K} - 10^8 \text{ K}$, respectively. Each of the superwinds has a power of $10^{41} \text{ erg s}^{-1}$ and a radius of 5 pc. The evolution of each wind starts from the adiabatic solution of CC85. The plots displays the whole computational grid: $100 \text{ pc} \times 1 \text{ kpc}$. The assumed metallicities were $Z = 10 Z_{\odot}$. The evolutionary times of the first four panels is $1.79 \times 10^5 \text{ yr}$, $4.82 \times 10^5 \text{ yr}$, $1.05 \times 10^6 \text{ yr}$ and $1.39 \times 10^6 \text{ yr}$, respectively.

or in temperature and velocity, and thus traces the presence of shocks and of rapid cooling zones.

The interaction of neighboring supersonic winds causes the immediate formation of their respective reverse shocks, and of a high pressure region right behind them. The pressure (and temperature) reaches its largest values at the base of the interaction plane, exactly where the reverse shocks are perpendicular to the incoming streams. The high pressure gas then streams into lower pressure regions, defining together with radiative cooling, how broad or narrow the high pressure zones, behind the reverse shocks, are going to be.

This also happens if cooling is fast enough, the oblique reverse shocks rapidly acquire a standing location, however in these cases, the loss of temperature behind the shocks is compensated by gas condensation, leading to narrow, dense and cold filaments. The drastic drop in temperature occurs near the base of the outflow, where the gas density is large and radiative cooling is exacerbated. The dense structures are then launched at considerable speeds (\sim several hundreds of km s^{-1}) from zones near the plane of the galaxy. These dense and cold structures are easy target to the UV radiation produced by the superstellar clusters and thus upon cooling and recombination are likely to become photoionized. Note however that as the free winds continue to strike upon these structures, even at large distances from their origin, the resultant cold filaments give the appearance of being enveloped by soft X-ray emitting streams.

All of these shocks are largely oblique to the incoming streams and thus lead to two major effects: a) partial thermalization and b) collimation of the outflow. These effects result from the fact that only the component of the original isotropic outflow velocity perpendicular to the shocks is thermalized, while the parallel component is fully transmitted and thus causes the deflection of the outflow towards the shocks. This leads both, to an efficient collimation of the outflow in a general direction perpendicular to the plane of the galaxy, and to a substantial soft X-ray emission associated with the dense filamentary structure, extending up to large distances (kpc) from the plane of the galaxy. In the figures one can clearly appreciate that the oblique shocks, confronting the originally diverging flows, lead to distinct regions where the gas acquires very different temperatures, allowing for radiation in different energy bands.

From our results it is clear that a plethora of structure, both in X-rays and in the optical line regime, as in M82, may originate from the hydrodynamical interaction of neighboring winds. The interaction leads to multiple standing oblique (reverse) shocks and crossing shocks able to collimate the outflow away from the plane of the galaxy. In our two dimensional simulations, these are surfaces that become oblique to the diverging streams and thus evolve into oblique shocks that thermalize only partly the kinetic energy of the winds causing a

substantial soft X-ray emission at large distances away from the galaxy plane. Surfaces that at the same time act as collimators, redirecting the winds in a direction perpendicular to the plane occupied by the collection of SSCs. Radiative cooling behind the oblique shocks leads, as soon as it sets in, to condensation of the shocked gas, and thus to the natural development of a network of filaments that forms near the base of the outflow, and streams away from the plane of the galaxy to reach kpc scales. Under many circumstances the filaments develop right at the base of the outflow and for all cases the prediction is that they are highly metallic. Hydrodynamic instabilities play also a major role on the filamentary structure. Nonlinear thin shell instabilities as studied by Vishniac (1994) as well as Kelvin Helmholtz instabilities, broaden, twist and generally shape the filaments as these stream upwards and reach kpc scales.

We thus postulate that if a collection of SSCs is sitting in a preferential plane, most of the injected energy would be channeled in a direction perpendicular to the plane of the host galaxy. This is achieved naturally as a consequence of the plethora of oblique and crossing shocks that redirect the initially isotropic winds. Collimation thus occurs without the need of a thick interstellar matter disk or a torus.

Our considerations point at a new set of possible parameters that profoundly impact the development of supergalactic winds. These are:

- The number and location of superstellar clusters within a galaxy nucleus.
- The intensity of star formation, or stellar mass in every superstellar cluster, which defines their mechanical luminosity,
- The age of the SSC, which impacts on the metallicity and thus on the cooling of the ejected matter.

All of these are relevant new parameters that may promote, as in M82, the inner structure of a supergalactic wind: the co-existence of X-rays and dense filaments, even at large distances from the sources of energy. Parameters that may promote self-collimation and with it the narrow waist of the biconical outflow. All of these features have been confirmed with full 3-D calculations, subject of a forthcoming communication. Note also that our results led to the full analysis of the HST data of M82 and to the discovery of 197 stellar clusters in the nucleus of M82 (see Melo et al. 2005).

4. Positive feedback from massive and compact SSC

The location of the threshold line in the \dot{E}_{SC} vs size (R_{SC}) diagram (see Figure 5), the line that defines whether or not a wind is inhibited, depends on several variables. It depends on the size of the star-forming region (R_{SC}) and the metallicity of the ejected gas, which has a strong impact on the cooling curve. It also depends on the assumed $\dot{E}_{SC}/\dot{M}_{SC}$ or adiabatic terminal speed (v_∞) of the wind. The latter is also bound to the usual assumption that the energy deposited by SN is always 10^{51} erg but the mass of the stars exploding within the cluster ranges from, say, $100 M_\odot$ to $8 M_\odot$ and so the injection speed (similar to v_∞) and the deposited amount of matter are also functions of time. Another factor that strongly affects the location of the threshold line is the thermalization efficiency (ϵ) which defines the fraction of the mechanical energy that upon thermalization, can be evenly spread within the cluster volume. Estimates of ϵ by several authors lead to values between 1 (Chevalier & Clegg; 1985) and 0.03 (see Melioli & Del Pino 2004 and references therein) and depends simply on the proximity of the sources undergoing winds and SNe, which through radiation may reduce the amount of energy available after thermalization. We have shown that there are three different types of solutions: SSCs far away from the threshold line (low mass, low energy clusters) undergo a quasi-adiabatic evolution well described by the Chevalier & Clegg (1985) solution. More energetic clusters are to have strongly radiative winds. Cooling hardly affects their velocity ($v_w \sim v_\infty$) and density distribution ($\rho_w \propto r^{-2}$), but their temperature instead of falling as $r^{-4/3}$, it falls rapidly to $T_w \sim 10^4$ K close to the SC boundary and the more so, the closer they are to the threshold line (see Figure 2). The strongly radiative winds around such clusters lead, compared to the adiabatic solution, to very much reduced X-ray envelope sizes. The third solution is for clusters above the threshold line. These would have their winds inhibited and as shown below, this turns them into very efficient positive feedback star-forming agents.

The facts above the threshold line are that radiative cooling drastically diminishes the sound speed c_{SC} and the pressure gradient across the SSC volume, inhibiting the possibility of a wind. Radiative cooling upsets then the stationary condition in which the deposited matter (\dot{M}_{SC}) has to equal, at all times, the amount of matter streaming out of the SC volume

$$\dot{M}_{SC} = 2\dot{E}_{SC}/v_\infty^2 = 4\pi R_{SC}^2 \rho_{SC} c_{SC} \quad (8)$$

where v_∞ is the resultant wind terminal speed in the absence of radiative cooling. As soon as this happens, the mass returned by the stars (\dot{M}_{SC}) begins to accumulate, promoting larger densities and an even faster cooling within the SSC volume. Following this trend, the

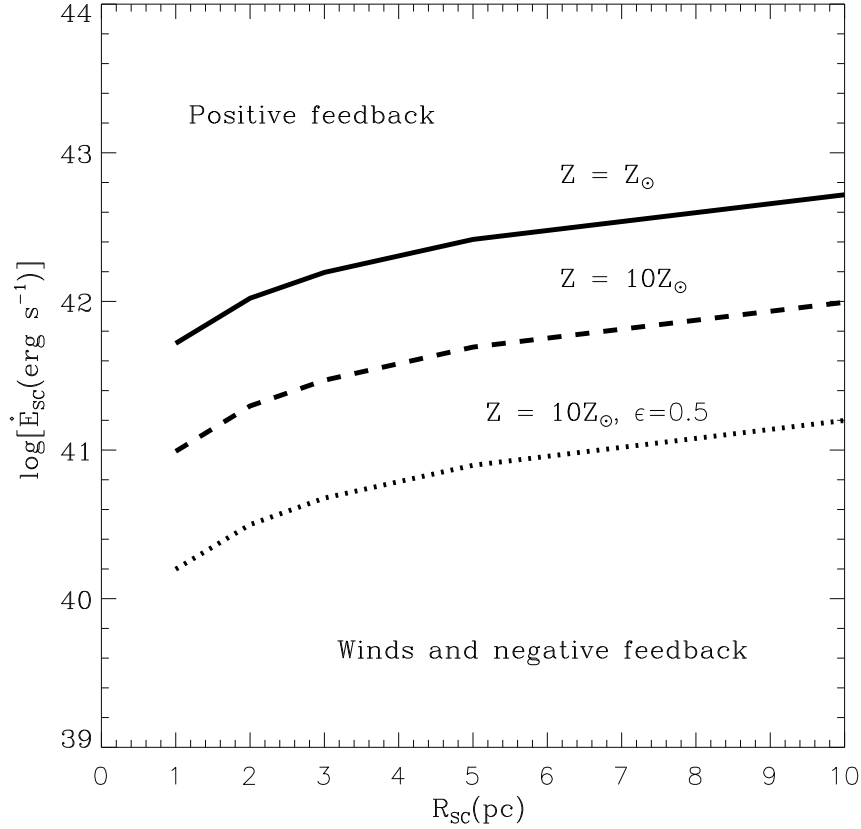


Fig. 5.— The threshold line. The location of the threshold line, the line that divides the \dot{E}_{SC} vs size (R_{SC}) diagram into two distinct areas. There the matter deposited within the SSC volume, through winds and SNE, ends up either streaming away as a stationary (adiabatic or radiative) wind (below the line) or it accumulates to end up steadily being driven into new episodes of star formation (above the line). Different locations of the threshold line, for an assumed full thermalization efficiency ($\epsilon = 1$), are display for an ejecta metallicity value equal to solar and ten times solar. The change in location for different values of ϵ is also indicated.

accumulated gas density ultimately fulfill the gravitational instability criterion causing the collapse into a new stellar generation.

For clusters above the threshold line, Figure 6 shows how the density of the accumulating gas ($\rho_{ac} = 3\dot{M}_{SC}t/4\pi R_{SC}^3$; where t the evolution time), grows as a function of time within the SSC volume, until the moment when the density of the accumulating gas exceeds the gravitational instability criteria

$$\rho_J \sim 2.3 \times 10^{-20} \left(\frac{T}{100K} \right) (R_{SC1})^{-2} \text{ g cm}^{-3} \quad (9)$$

where ρ_J is the Jeans density and R_{SC1} is the SSC radius in pc units. At that moment, when $\rho_{ac} = \rho_J$ collapse will inevitably proceed. Note that for a given SSC (with a fixed volume), ρ_{Jeans} is only a function of temperature and this is set, at least initially, by photoionization.

For massive clusters the initial ample supply of UV photons exceeds at first the number of recombinations within the volume occupied by the reinserted gas and the resultant HII region, given the large metallicities of the ejecta, is here assumed to rapidly approach an equilibrium temperature $T_{HII} \sim$ a few 10^3 K. At these temperatures the sound speed (< 10 km s $^{-1}$) remains well below the escape speed and the reinserted gas would inevitably continue to accumulate to rapidly (within 1.5×10^6 yr) reach the value of the Jeans density for a gas at say, $T_{HII} = 5000$ K, and collapse into a new stellar generation. The event gives rise to a new phase of matter accumulation, which once more will rapidly approach ρ_J (for $T = 5000$ K) and undergo collapse within a free-fall time, of the order of 10^5 yr, while transforming $\sim 2 \times 10^5 M_{\odot}$ into stars. All stellar generations resultant from mass accumulation within the SSC volume have here been assumed to also acquire a Salpeter IMF with similar upper and lower mass limits as those imposed to the main superstellar cluster, and their resultant properties (mechanical energy and UV photon output) have been added to those produced by the main cluster.

A few, almost identical, stellar generations are expected from the accumulation process (solid rising lines in Figure 6), every time that the accumulated gas density ρ_{ac} reaches $\rho_J(5000K)$ (dashed line in Figure 6). The situation changes slightly when the number of ionizing photons (N^0), despite the added contribution of secondary stellar generations, becomes insufficient to fully ionize the matter accumulated within the star cluster volume. This is due to the evolution of the main cluster, whose UV photon output begins to fall as t^{-5} after ~ 3.5 Myr. Figure 6 shows ρ_{HII} (thin solid line), the maximum density within the SSC volume that can be supported fully ionized by the UV radiation produced by the evolving cluster ($\rho_{HII} = (3N^0\mu^2/(4\pi R_{SC}^3\beta))^{0.5}$; where $\mu = 1.4m_H$ and β , the recombination coefficient to to all levels above the ground level = 2.59×10^{-13} cm $^{-3}$ s $^{-1}$). During the accumulation process, once ρ_{ac} exceeds ρ_{HII} , the ionized volume begins to shrink to end up as a collection

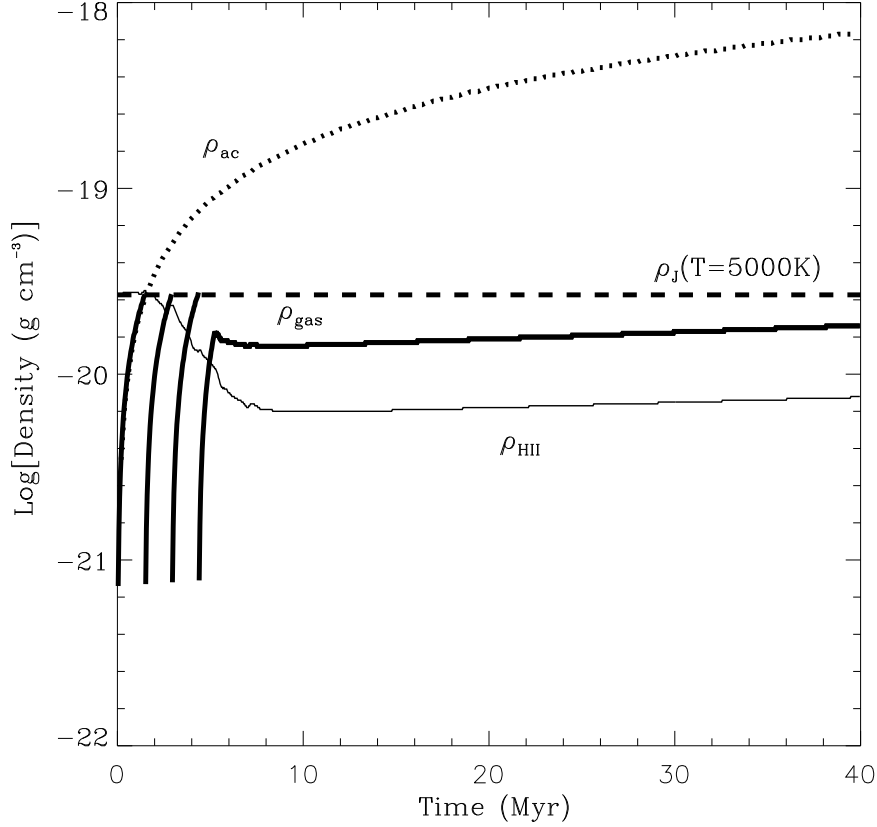


Fig. 6.— Positive star-forming feedback. The figure shows the rapid growth of the reinserted gas density within the SSC volume (rising solid lines), interrupted as it reaches the gravitational instability criterion (ρ_J), leading to a new stellar generation and to a new phase of matter accumulation. The situation changes slightly as the available photon flux becomes unable to sustain all the SSC volume fully ionized, allowing for recombination and further cooling of the recombined matter, and thus to a much lower limit of the Jeans instability criterion. This allows the accumulation time to become comparable to the free-fall time, establishing a new stationary condition in which $\dot{M}_{SC} = \text{SFR}$. The density value (ρ_{gas}) required for this condition is also indicated in the figure as well as the maximum density value (ρ_{HII}) that can be supported fully ionized within the SSC volume, with the available UV photon flux.

of ultra compact HII regions around the most massive stars left within the cluster, while the bulk of the ejected material, now recombined, continues to cool, approaching rapidly a temperature ~ 100 K. The characteristic cooling time ($t_\Lambda = 3kT/2\Lambda n$; where Λ is the cooling rate, a function of T and Z) is also very small, $\sim 1.5 \times 10^5$ yr, and is to become even shorter as matter continues to accumulate. Matter is at all times uniformly replenished within the whole SSC volume, and thus the gas density presents an almost uniform value. However, the accumulating gas now has two different temperatures (T_{HII} and 100 K) and as ρ_{ac} grows and the fraction of the ionized volume ($f_{HII} = (3N^0\mu^2)/(4\pi R_{SC}^3\beta\rho_{ac}^2)$) shrinks, the size of cold condensations (at 100 K) able to become gravitationally unstable and their free-fall time also become smaller.

The drop in the number of ionizing photons and the consequent growth of the neutral volume, lead then to a second important condition in which the characteristic accumulation time

$$\tau_{ac} = \frac{4}{3}\pi\rho_{gas}R_{SC}^3(1 - f_{HII})/\dot{M} \quad (10)$$

becomes equal to the free-fall time

$$t_{ff} = \sqrt{\frac{3\pi}{32G\rho_{gas}}}, \quad (11)$$

This condition defines ρ_{gas} , the density above the Jeans instability limit for a neutral condensation at 100 K ($\rho_J(100K)$):

$$\rho_{gas} = \left(\frac{27\dot{M}^2}{512\pi G(1 - f_{HII})}\right)^{1/3} R_{SC}^{-2} = 1.15 \times 10^{-18} \left(\frac{\dot{M}}{1M_\odot yr^{-1}}\right)^{2/3} \left(\frac{R_{SC}}{1pc}\right)^{-2} \quad (12)$$

and thus once ρ_{ac} becomes equal to ρ_{gas} , a new stationary solution becomes possible.

Everything happens very rapidly, compared to the evolution time-scale of the parental cluster (~ 40 Myr), and almost at the same time. The ejected matter is thermalized within the SSC volume and immediately begins to cool. At the same time that it accumulates making cooling even faster. This allows it to rapidly reach the required ρ_{gas} value, above the Jeans instability limit, that warrants its collapse in a similar time-scale, while the collapsing material is replenished by the newly ejected matter. When this happens, the mass deposition rate from the cluster becomes equal to the rate of star formation. Gravitational collapse and star formation within the star cluster volume and with the matter injected by all sources, drive in this way a new stationary condition through a new era of quasi-continuous star formation in which \dot{M}_{SC} is now equal to the star formation rate (SFR). Further details describing this phase are given in Tenorio-Tagle et al. 2005.

5. Conclusions

Superstellar clusters are certainly the main mode of massive star formation in starburst and interacting galaxies. We have reviewed here how is that they work and the possible impact that they may have into the surrounding ISM. We have revised the assumptions of Chevalier & Clegg (1985) dealing with thermalization and the flow requirements to establish a stationary superwind emanating from these sources. We have also emphasized the importance of radiative cooling and how does it affect the superwind X-ray envelopes.

Calculations in the literature have left clear the fact that single energy sources lead to superbubbles and supershells. However, to produce a supergalactic wind with a detailed inner structure as in M82, multiple sources, seem to be required.

We have also shown that a straight forward extrapolation towards the most massive and compact coeval clusters is not valid. When radiative cooling becomes significant within the SSC volume itself, then instead of driving a superwind able to disperse the surrounding ISM and even channel its way into the IGM, events that have make them been regarded as negative feedback agents, they become in fact extreme examples of positive star formation feedback.

Massive and compact coeval clusters appear in the \dot{E}_{SC} vs cluster size diagram above the threshold line, in the region where radiative cooling inhibits the development of stationary superwinds. In such cases the matter reinserted, through stellar winds and supernovae, is unable to escape and after a short phase of matter accumulation, a new stationary solution in which \dot{M}_{SC} becomes equal to the SFR is rapidly met. A positive feedback condition in which new stellar generations result in situ, from the collapse of the matter reinserted by the sources evolving within the star cluster volume.

The massive concentrations imply a high efficiency of star formation which permits even after long evolutionary times the tight configuration that characterizes them, despite stellar evolution and its impact through photo-ionization, winds and supernova explosions, believed to efficiently disperse the gas left over from star formation. It is thus the self-gravity that results from the high efficiency what keeps the sources bound together.

The secondary star formation process while causing a faster mass deposition rate, drives the SFR to grow from 0.1 to 0.25 $M_{\odot} \text{ yr}^{-1}$ over the parent cluster supernova phase (~ 40 Myr). The continuous reprocessing of the ejected material leads effectively to a continuous transformation of the high mass stars into a low mass ($\leq 8 M_{\odot}$) population, keeping constant the total mass of the stellar component.

A central issue, regarding ISM studies, is the fact that the more massive and compact

clusters (as those detected by HST and other large ground-based telescopes), are unable to generate superwinds and shed their metals into the ISM or the IGM. Their evolution leads to many stellar generations and thus to a mixture of stellar populations, all contaminated by the products from former stellar generations. An exacerbated episode of star formation that leaves no trace of its evolution in the ISM.

GTT acknowledges financial support from the Secretaría de Estado de Universidades e Investigación (España) ref: SAB2004-0189 and the hospitality of the Instituto de Astrofísica de Andalucía (IAA, CSIC) in Granada, Spain. This study has been partly supported by AYA2004-08260-CO3-O1 from the Spanish Consejo Superior de Investigaciones Científicas.

REFERENCES

- Cerviño, M. & Mas-Hesse, M. 1994, *A&A* 284, 749
- Chevalier, R.A. & Clegg, A.W. 1985, *Nature*, 317, 44
- Colina, L., Gonzalez-Delgado, R., Mas-Hesse, M. & Leitherer, C. 2002 *ApJ* 579, 545
- Devine, . & Bally, J. 1999 *ApJ* 510, 197
- Ho, L. C. 1997, *Rev.MexAA*, Conf. Ser. 6, 5
- Johnson, K. E., Kobulnicky, H. A., Massy, P. & Conti, P. S. 2001, *ApJ* 559, 864
- Kobulnicky, H. A. & Johnson, K. E. 1999, *ApJ* 527, 154
- Larsen, S. S. & Richtler, T. 2000, *A&A* 354, 836
- Lamers, H., et al., 2004, in *ASP Conf. Ser.* 322, The formation and evolution of massive young star clusters, eds. H.J.G.L.M. Lamers, L.J. Smith & A. Nota (San Francisco: ASP)
- Leitherer, C., Schaerer, D., Goldader, J.D. et al. 1999, *ApJS*, 123, 3
- Melioli, C. & de Gouveia Del pino E. M. 2004 *A&A* 424, 817
- Melo, V., Muñoz-Tuñón, C., Maiz-Apellaniz, J. & Tenorio-Tagle G. 2005 *ApJ* 619, 270
- Meynet, G. & Maeder, A. 2002, *A&A*, 390, 561.

- Ohyama, Y. et al. 2002, in the Proceedings of the IAU 8th Asian Pacific Regional Meeting Vol 2. Eds. S. Ikeuchi, J. Hearnshaw, T. Hanawa (Tokio ASJ), 285.
- Pasquali, A., Gallagher, J. S. & de Grijs, R. 2004 *A&A* 415, 103
- Raymond, J. C., Cox, D. P. & Smith, B. W. 1974 *ApJ* 204, 290.
- Silich, S. & Tenorio-Tagle G. 2001 *ApJ* 552, 91.
- Silich, S. & Tenorio-Tagle G. Muñoz-Tuñón, C. 2003, *ApJ*, 590, 796.
- Silich, S., Tenorio-Tagle G. & Rodríguez González, A. 2004, *ApJ*, 610, 226.
- Silich, S., Tenorio-Tagle G., Terlevich, R., Terlevich, E. & Netzer, H. 2001, *MNRAS*, 324, 191
- Strickland, D.K., Ponman, T. J. & Stevens, I. R., 1997, *A&A*, 320, 378
- Strickland, D.K. & Stevens, I. R., 2000, *MNRAS*, 314, 511
- Suchkov, A. A., Balsara, D. S., Heckman, T. M. Leitherer, C. 1994, *ApJ*, 463, 528
- Tenorio-Tagle, G. & Muñoz-Tuñón, C. 1997, *ApJ*, 478, 134
- Tenorio-Tagle, G. & Muñoz-Tuñón, C. 1998, *MNRAS*, 293, 299
- Tenorio-Tagle, G., Silich, S. & Muñoz-Tuñón, C. 2003, *ApJ*, 597, 279
- Tenorio-Tagle, G., Silich, S., Rodríguez-González A. & Muñoz-Tuñón, C., 2005, *ApJ* 620, 217.
- Tomisaka, K. & Ikeuchi, S. 1988 *ApJ*, 330, 695.
- Walcher, C.J., van der Marel, R.P., McLaughlin, D., Rix, H.-W., Böker, T., Häring, N., Ho, L.C., Sarzi, M. & Shields, J.C. 2005, *ApJ*, 618, 237
- Whitmore, B. C., Zhang, Q., Leitherer, C., Fall, M. S., Schweizer, F. & Miller, B. W., 1999, *AJ*, 118, 1551

This figure "gtt4.gif" is available in "gif" format from:

<http://arxiv.org/ps/astro-ph/0506124v1>